NASA Technical Memorandum 110221

SIMULATION OF THE PHOTOGRAMMETRIC APPENDAGE STRUCTURAL DYNAMICS EXPERIMENT

Richard S. Pappa
Michael G. Gilbert
Sharon S. Welch

Langley Research Center
Hampton, Virginia 23681-0001

November 1995

National Aeronautics and
Space Administration
Langley Research Center
Hampton, Virginia 23681-0001

SIMULATION OF THE PHOTOGRAMMETRIC APPENDAGE STRUCTURAL DYNAMICS EXPERIMENT

Richard S. Pappa, Michael G. Gilbert, and Sharon S. Welch
NASA Langley Research Center
Hampton, VA 23681

ABSTRACT

The Photogrammetric Appendage Structural Dynamics Experiment (PASDE) uses six video cameras in the Space Shuttle cargo bay to measure vibration of the Russian Mir space station Kvant-II solar array. It occurs on Shuttle/Mir docking mission STS-74 scheduled for launch in November 1995. The objective of PASDE is to demonstrate photogrammetric technology for measuring "untargeted" spacecraft appendage structural dynamics. This paper discusses a pre-flight simulation test conducted in July 1995, focusing on the image processing aspects. The flight camera systems recorded vibrations of a full-scale structural test article having grids of white lines on black background, similar in appearance to the Mir solar array. Using image correlation analysis, line intersections on the structure are tracked in the video recordings to resolutions of less than 0.1 pixel. Calibration and merging of multiple camera views generated 3-dimensional displacements from which structural modal parameters are then obtained.

INTRODUCTION

Over the years, NASA and its contractors have investigated options for measuring the structural dynamic characteristics of the International Space Station (ISS) during assembly and operation in low Earth orbit. These measurements are used to improve structural analytical models and modeling techniques, modify flight operations or control systems if unexpected dynamics occur, and monitor structural health using modal parameters, among other uses (Refs. 1-4). Structural vibrations are usually measured with accelerometers. However, it is difficult to mount accelerometers on ISS solar arrays and thermal radiators, and also to transmit the signals back across rotating joints. Photogrammetry is an attractive alternative for these situations.

Photogrammetry is the science of measuring the dimensions or locations of objects in photographs or in other types of images (Refs. 5-6). When applied to a sequence of images, photogrammetry can track the motion (or vibration) of structures (Refs. 7-9). In most applications, bright light sources or reflective targets are placed on the object to simplify tracking. Target locations are determined by simply calculating centers of brightness (centroids), which can be performed at real-time video rates with modern computer hardware (Ref. 10). With operating ISS solar arrays and radiators, however, it is preferable to avoid installation of light sources or reflectors if possible.

The Photogrammetric Appendage Structural Dynamics Experiment (PASDE) will demonstrate that naturally occurring features of "untargeted" solar arrays, such as line intersections and/or segments, can be accurately tracked using charge-coupled device (CCD) video cameras and digital image processing techniques (Refs. 11-12). Structural modal parameters are then identified from the resulting time histories. PASDE uses six cameras stored in three Hitchhiker canisters in the Space Shuttle cargo bay on docking mission STS-74 to record vibrations of the lower Mir Kvant-II solar array. Figure 1 shows the experiment configuration. One camera in each canister aims at the upper portion (root) of the solar array while the other camera aims at the lower portion (tip), with some overlap.

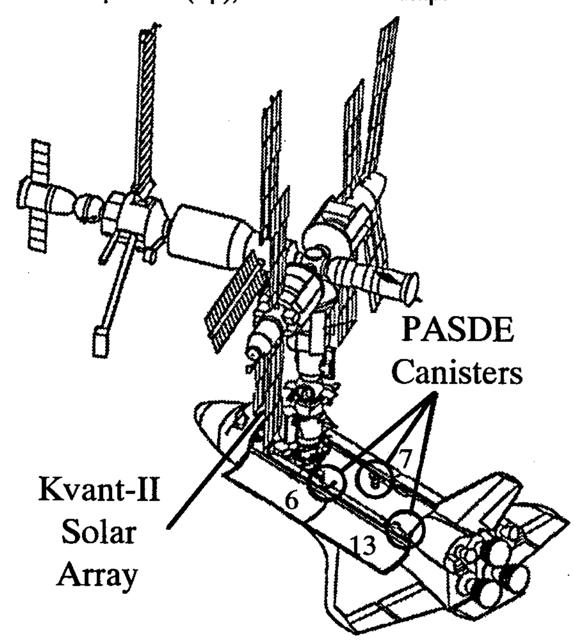

Fig. 1 - STS-74 Shuttle/Mir Configuration

The Kvant-II solar array will be video taped by all six cameras simultaneously during Shuttle-Mir docking, day/night and night/day orbital transitions (to measure thermal response), as well as during scheduled firings of the Shuttle primary reaction control thrusters. A total of two hours of video tape is available for each camera for these purposes. A limited amount of live video will also be received during the experiment to optimize video quality. All data analysis occurs after the flight.

This paper discusses a pre-flight simulation test of PASDE, focusing on the digital image processing aspects. The test occurred in a clean room at the Kennedy Space Center in July 1995. A vibrating, full-scale test article was video taped by all six flight cameras simultaneously. The structure has grids of white lines painted on black background, similar in appearance to the Mir solar array. In each test the structure was deflected by hand and then allowed to vibrate freely. The arrangement of the cameras (in their canisters) duplicated the flight geometry.

The next two sections of the paper briefly describe the cameras, the test article, and the test procedure. The third section summarizes the three steps involved in data analysis for PASDE. The fourth section is the main topic of the paper, namely, digital image processing for tracking solar array motion in video recordings. An image correlation procedure with interpolation is described and illustrated in detail. The procedure successfully tracked line intersections on the test article to resolutions of less than 0.1 pixel. The paper concludes with sample modal identification results obtained using these photogrammetric data.

CAMERAS

PASDE uses six monochrome CCD video cameras with individual Hi-8 mm recorders. Two cameras and two recorders are contained in each of three Hitchhiker canisters. The canisters mount near the sidewalls of the Space Shuttle cargo bay in Bay Nos. 6, 7, and 13 (Fig. 1). Canisters 6 and 13 are on the port side of the orbiter while canister 7 is on the starboard side. Table 1 shows the assigned camera numbers. Most of the data discussed in this paper is from Camera No. 3.

All six cameras are Pulnix model TM-9701 units with standard RS 170 composite video output. Each camera has a fixed 50 mm lens and a motorized iris. The pointing direction and focus of each camera are set before launch, but the iris is adjustable by ground command as lighting conditions warrant.

Camera No.	Canister	Root	Tip
1	6	√	
2	6		√
3	7	√	
4	7		√
5	13	√	
6	13		√

Table 1 - Camera Numbers

With the solar array rotated as shown in Fig. 1, all cameras view the same side of the structure. The vertical distance from the cameras to the tip of the array is approximately 24 ft. The near edge of the solar array is located approximately 15 ft outboard of Canister 6. Each camera sees about one-half of the array, which is 33 ft in length. Note that the Mir space station on mission STS-74 is rotated counter-clockwise from the longitudinal axis of the Shuttle. This rotation angle is 25 degrees.

TEST ARTICLE AND TEST PROCEDURE

Figure 2 is a sketch of the test article, and Figs. 3 and 4 show video images from Cameras 3 and 4. The structure consists of two rigid 4 ft x 4 ft plates spaced 10 ft apart by angle iron. A grid of white lines on black background covers each plate. The line spacing is 4 inches. The 18 line intersections marked in Fig. 2 are tracked in the data analysis. The terminology "targets" is given to these 18 intersections.

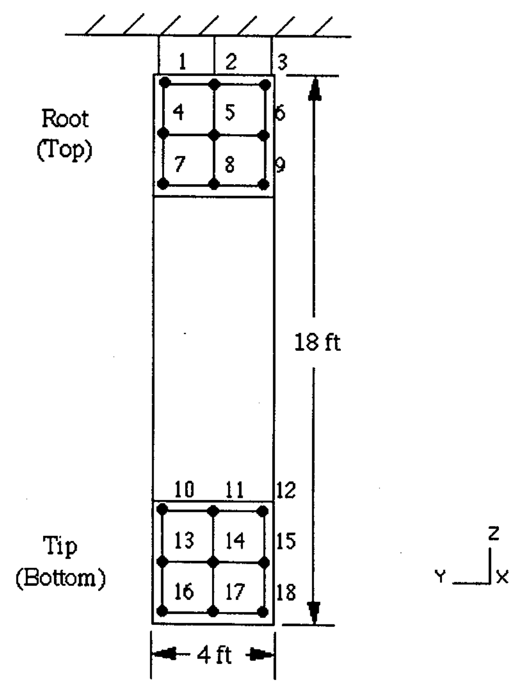

Fig. 2 - Test Structure

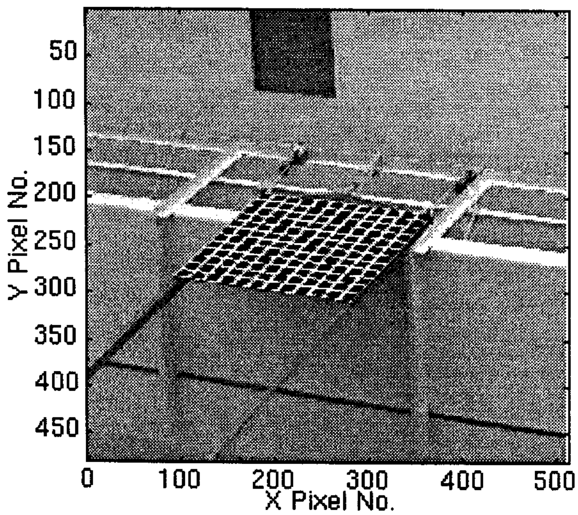

Fig. 3 - Camera 3 Image (Root 7)

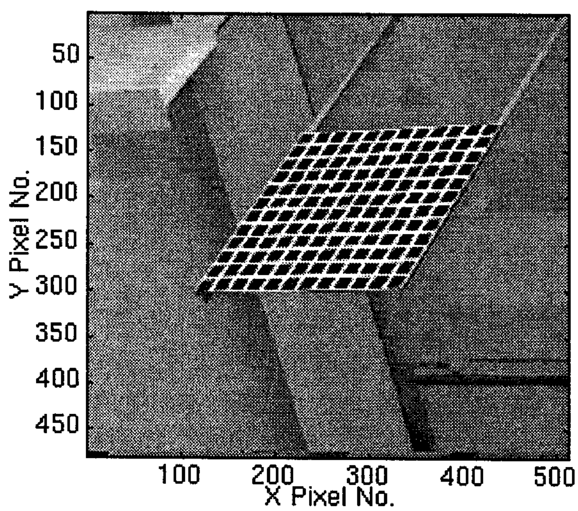

Fig. 4 - Camera 4 Image (Tip 7)

As seen in Fig. 3, the test article was attached to the railing of an overhead walkway. The canisters were then moved on the floor of the room to their correct locations and orientations. This procedure permitted the camera locations and pointing directions relative to the structure to closely match their flight values. Theodolite measurements validated all physical dimensions. Note that the test structure is 18 ft long (Fig. 2) whereas the Mir solar array is 33 ft long. The test structure was sized to place the center of each grid (i.e., Targets 5 and 14) at the center of the viewing areas of the root and tip cameras, respectively.

Simple manual excitation generated free-decay vibrations. The tip of the structure was displaced using three attached cords, and then released. All results presented in this paper are for an out-of-plane excitation test with an initial tip displacement of about 5 inches. Each test lasted approximately one minute, with the video tape recorders for all six cameras running simultaneously. The Hitchhiker canisters provide time code signals allowing synchronization of the individual tapes during data analysis.

DATA ANALYSIS STEPS FOR PASDE

Data analysis consists of three distinct steps: 1) tracking of selected features in the video images using digital image processing, 2) transformation of these "target" time histories from 2-D image coordinates to 3-D physical coordinates, and 3) structural modal identification using the resulting free-decay histories. The first step is considered to be the most difficult in PASDE because only naturally occurring structural features such as line intersections and/or segments are tracked. Also, fluctuations of image contrast (affecting the video signal-to-noise ratio) may occur due to shadowing or other lighting variations in space. In the pre-flight preparation for PASDE, this step of the data analysis has been given the most attention because of its difficulty and importance. The information contained in the following section of the paper is a result of this effort.

DIGITAL IMAGE PROCESSING

Digitization

Although CCD sensors contain an array of discrete light-sensing elements (pixels), the images are outputted from the sensors in continuous, analog form for video recording and display (RS 170 format). Thus, the video recordings must be redigitized before analysis. Note that the number of pixels of the sensor is not necessarily equal to the number of pixels of the redigitized images. In PASDE, the cameras have CCD arrays of 486 x 764 pixels (V x H), whereas the digitized images have 480 x 512 pixels.

The video recordings from the simulation test were digitized at the full rate of 30 frames/sec, providing approximately 1800 images per camera, per test. Each digitized image of 480 x 512 pixels has 8 bits of intensity information, for a storage requirement of approximately 1/4 Mbyte per image. The intensity of each pixel is an integer value ranging from 0 to 255, where 0 is pure black and 255 is pure white. Intermediate values represent various shades of gray.

Cross-Correlation Analysis

Correlation of images allows matching of particular features in two or more separate views (Ref. 12). Example applications reported in the literature include matching of aerial photographs (Ref. 13) and displacement measurement of speckle patterns (Ref. 14). The cross-correlation function measures the degree of similarity of two images at various amounts of shifting of one image relative to the other. Maximum correlation occurs at the x-y shift values where the two images are most similar. By finding the point of maximum correlation, the change of position of a "target" (i.e., any identifiable feature) from one image to the other is determined. Applying this fact to a sequence of images generates a time history of the motion.

Referring to Fig. 5, the cross-correlation function of Images A and B is calculated by shifting Image A over the range of +/- M pixels in the x direction and +/- N pixels in the y direction from its center position, as follows:

$$R(m,n)=\frac{\sum_x\sum_y\left[A(x-m,y-n)-\bar{A}\right]\left[B(x,y)-\bar{B}\right]}{\left[\sum_x\sum_y\left[A(x-m,y-n)-\bar{A}\right]^2\sum_x\sum_y\left[B(x,y)-\bar{B}\right]^2\right]^{1/2}}$$

where $\bar{A}$ is the average intensity of image A and $\bar{B}$ is the average intensity of image B in the region coincident with A. The shift values $-M \le m \le M$ and $-N \le n \le N$ must be somewhat larger than the distance that the target has moved from Image A to Image B.

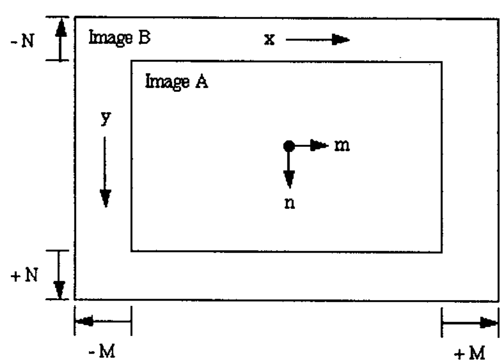

Fig. 5 - Correlation of Images A and B

In practice, correlating a fixed starting video frame ("A") with a series of succeeding frames ("B") is preferable to correlating adjacent pairs of frames and accumulating the total amount of shift. Summing a large number of small shifts was found to be susceptible to accumulated error, causing drift in the target positions.

<u>Target-Tracking Results</u>

The remainder of this section shows example target-tracking results. Most of the target time histories obtained in this application using cross-correlation of images are similar in quality to those shown.

Figure 6 shows the starting position of Target 8 in Frame 1 of Camera 3. This image, referred to as the "correlation region of Target 8," corresponds to Image A of Fig. 5. The size of the correlation region is selected to include characteristic contrast patterns in both the x and y directions. The region centers on the starting target position (the 'x'), which is selected manually by cursor.

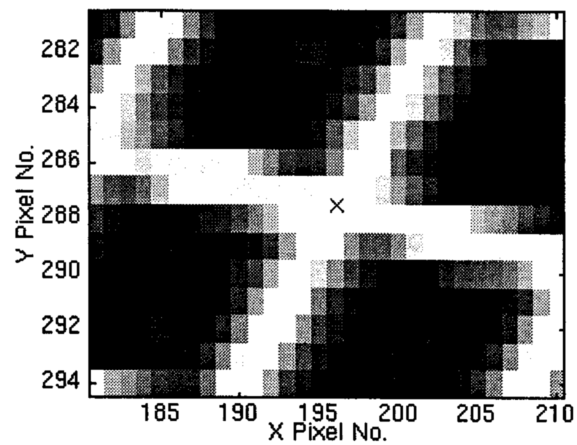

Fig. 6 - Starting Position of Target 8 in Frame 1 of Camera 3

Figure 7 shows the search area in video frame No. 20 for this target, corresponding to Image B of Fig. 5. It centers on the last calculated position of Target 8, which in this case is the position calculated in frame No. 19. The search area is 8 rows and 8 columns larger in size than the correlation region, Fig. 6 (i.e., M = N = 4). The 'x' in Fig. 7 is the calculated position of Target 8 in frame 20, using the procedure described below.

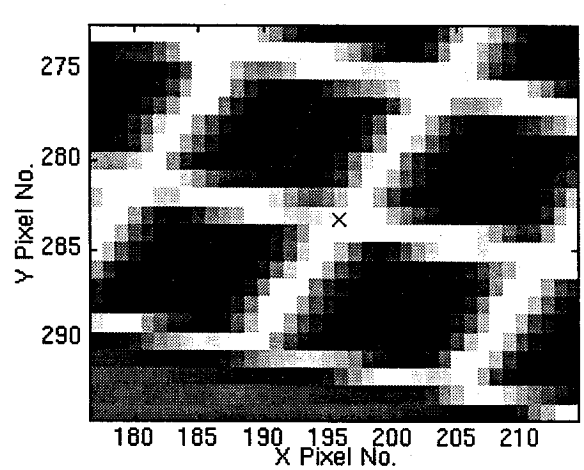

Fig. 7 - Search Area of Target 8 in Frame 20 of Camera 3

The cross-correlation function of Figs. 6 and 7 appears in Fig. 8. The pixel of maximum intensity occurs at x shift and y shift values of 0 and -4, respectively. Note that the basic correlation function, R(m,n), has a spatial resolution of 1 pixel. However, the correlation function itself inherently has much higher resolution if other pixels in the neighborhood of the pixel of maximum intensity are considered.

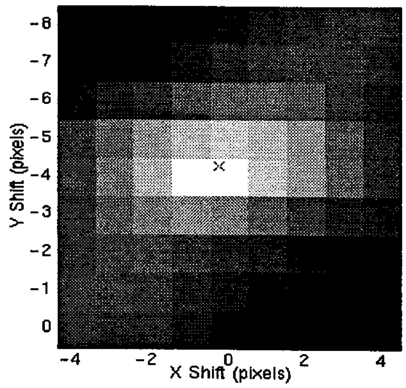

Fig. 8 - Cross-Correlation of Target 8 From Frame 1 to Frame 20 (Camera 3)

Several methods of achieving subpixel resolution of the correlation function were investigated. An effective yet efficient approach is as follows: Fit a cubic spline function through 5 values of R(m,n) centered along both the row and column of maximum correlation. Evaluate the spline function every 0.001 pixel and use the position of its maximum value as the peak correlation location. Figures 9 and 10 show results obtained in this manner for the correlation function in Fig. 8. The coordinates of the 'x' in Fig. 8 correspond to these interpolated results.

Note that there are two curves plotted in Figs. 9 and 10. The smooth curve is the spline function and the other is simply the connection of the data points by straight lines.

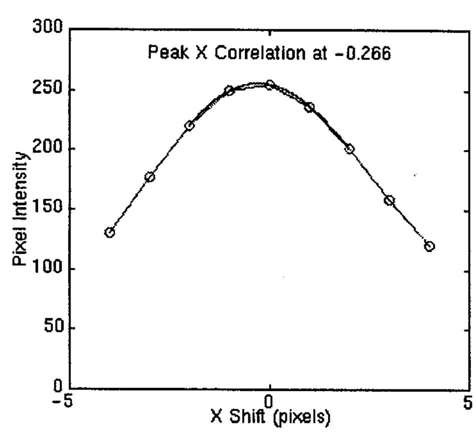

Fig. 9 - 5-Point Cubic Spline Fit Along Row of Maximum Correlation of Fig. 8

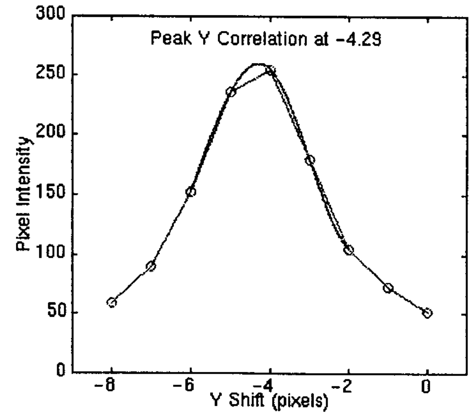

Fig. 10 - 5-Point Cubic Spline Fit Along Column of Maximum Correlation of Fig. 8

Figure 11 shows the y-direction time history of Target 8 obtained by this approach. The quality of the results for Targets 4 through 18 is similar to that shown for Target 8. Results for Targets 1 through 3, however, are considerably noisier because of the small amplitude of motion near the root of the test structure.

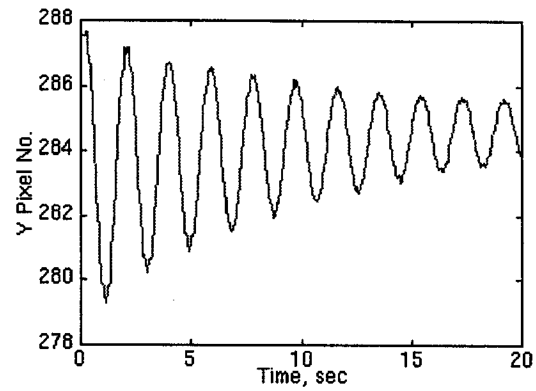

Fig. 11 - Y-Pixel Time History of Target 8 for Camera 3

Subpixel Measurement Resolution

The effective resolution of the spline-function interpolation method is determined by examining the results at locations having very small vibration amplitudes, such as at Target 2. Figure 12 shows both x- and y-direction results for this target. The predominant vibration frequency of approximately 0.5 Hz is visible in both time histories although the peak-to-peak amplitude is much less than 1 pixel in both directions. For these results, the rms measurement noise floor is estimated to be approximately 0.03 pixel in the x direction and 0.01 pixel in the y direction (image coordinates).

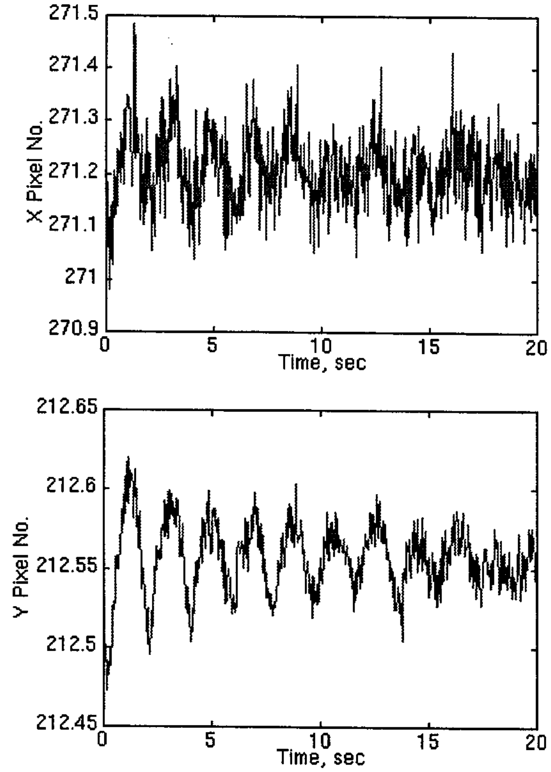

Fig. 12 - Comparison of X and Y Measurement Resolutions of Target 2 for Camera 3

Subpixel measurement resolution is an important parameter in photogrammetry, and considerable research is devoted to its improvement. Reference 15 provides a good overview of this subject.

Correlation Coefficients

Other important information is found in the time history of the correlation coefficient. The correlation coefficient is the peak value of the cross-correlation function. These results for Target 2 are shown in Fig. 13.

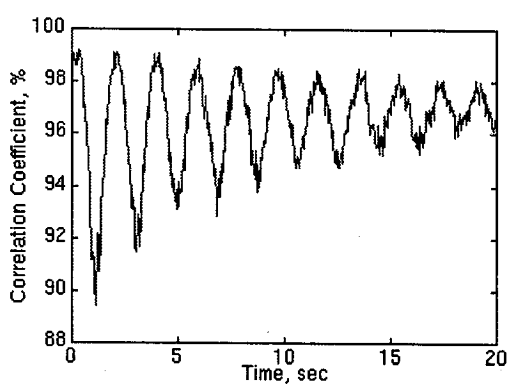

Fig. 13 - Correlation Coefficient Time History of Target 2 for Camera 3

Although the correlation coefficient is quite high throughout the entire history (>90% is generally considered to be "good" correlation), there are regular oscillations at the 0.5 Hz vibration frequency. The dips in correlation occur when the structure has moved the furthest from its initial position at time zero. These reductions of correlation result from a slight change in image intensity, as well as a slight rotation of the grid lines in the image frames, as the structure swings back and forth.

MODAL IDENTIFICATION

After converting the target time histories in x,y image coordinates to x,y,z object coordinates (this step is beyond the scope of this paper -- see Ref. 5 for details), the free-decay data are suitable for structural modal identification purposes. Recall that all results shown in this paper are for an out-of-plane excitation test with an initial tip displacement. Therefore, the first out-of-plane bending mode dominates measured responses. The frequency of this mode is clearly observed to be approximately 0.5 Hz.

The data for Targets 1 through 18 are analyzed using the Eigensystem Realization Algorithm (Ref. 16). A natural frequency of 0.524 Hz and damping factor of 2.3% are found, together with the mode shape shown in Fig. 14. The overall accuracy of the photogrammetric procedures described in this paper is clear.

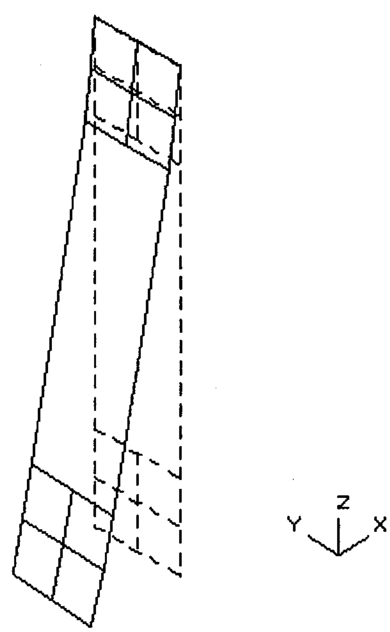

Fig. 14 - Identified Mode at 0.524 Hz

CONCLUSIONS

Due to the difficulty of installing accelerometers on the solar arrays and radiators of the International Space Station, photogrammetry using CCD video cameras is being studied as an alternative measurement approach. The simplest way to acquire these data is to track the motion of naturally occurring structural features such as line intersections and/or line segments. The Photogrammetric Appendage Structural Dynamics Experiment (PASDE) flies on Shuttle/Mir docking mission STS-74 in November 1995 to demonstrate the feasibility of this approach. Six CCD video cameras in the Shuttle cargo bay will measure vibrations of the Mir Kvant-II solar array for various excitation events.

The pre-flight simulation test discussed in this paper verifies experiment readiness. The accuracy of results, such as sub-pixel measurement resolutions less than 0.1 pixel, meets expectations. These findings translate into expected measurement resolutions in PASDE of less than 0.1 inches.

ACKNOWLEDGEMENT

The authors thank Martha Demeo of Vigyan, Inc. of Hampton, Virginia, for creating and managing the image data files used in this project.

REFERENCES

1. Cooper, P. A. and Johnson, J. W., "Space Station Freedom On-Orbit Modal Identification Experiment -- An Update," *Second USAF/NASA Workshop on System Identification of Precision Space Structures*, March 1990, pp. 683-714.

2. Blelloch, P., Engelhardt, C., and Hunt, D. L., "Simulation of On-Orbit Modal Tests of Large Space Structures," *Proceedings of the 8th IMAC*, Jan. 1990, pp. 926-932.

3. Teague, H. and Parkinson, B. W., "Translation, Rotation, and Vibration Control of Large Space Structures Using Self-Differential GPS," AAS paper 93-017, Feb. 1993.

4. Kim, H. M. et al, "Health Monitoring of Large Structures," *Sound and Vibration*, Vol. 29, No. 4, 1995, pp. 18-21.

5. Slama, C. C., Theurer, C., and Henriksen, S. W., eds., *Manual of Photogrammetry*, Fourth Edition, American Society of Photogrammetry, Falls Church, VA, 1980.

6. Gruen, A. and Kahmen, H., eds., *Proceedings of the Conference on Optical 3-D Measurement Techniques*, Federal Institute of Metrology and Surveying, Vienna, Austria, Sept. 1989.

7. Walton, J. S., ed., "Image-Based Motion Measurement," *Proceedings of the Society of Photo-Optical Instrumentation Engineers,* Vol. 1356, Aug. 1990.

8. Gruen, A. and Baltsavias, E., eds., "Close-Range Photogrammetry Meets Machine Vision," *Proceedings of the Society of Photo-Optical Instrumentation Engineers,* Vol. 1395, Sept. 1990.

9. Brumfield, M. L. et al, "Orbital Dynamics of the OAST-1 Solar Array Using Video Measurements," AIAA Paper 85-0758, April 1985.

10. El-Hakim, S. F., "Real-Time Image Metrology With CCD Cameras," *Photogrammetric Engineering and Remote Sensing*, Vol. 52, No. 11, Nov. 1986, pp. 1757-1766.

11. Gilbert, M. G., Welch, S. S., and Moore, C. L., "The Photogrammetric Appendage Structural Dynamics Experiment," NASA CP-3310, Sept. 1995, pp. 73-82.

12. Gonzalez, R. C. and Wintz, P., *Digital Image Processing*, Second Edition, Addison-Wesley Publishing Co., Reading, MA, 1987.

13. Gotashby, A., Stockman, G. C., and Page, C. V., "A Region-Based Approach to Digital Image Registration With Subpixel Accuracy," *IEEE Transactions on Geoscience and Remote Sensing*, Vol. 24, No. 3, 1986, pp. 390-399.

14. Oulamara, A., Tribillon, G., and Duvernoy, J., "Subpixel Speckle Displacement Measurement Using a Digital Processing Technique," *Journal of Modern Optics*, Vol. 35, No. 7, 1988, pp. 1200-1211.

15. West, G. A. W. and Clarke, T. A., "A Survey and Examination of Subpixel Measurement Techniques," *Proceedings of the Society of Photo-Optical Instrumentation Engineers,* Vol. 1395, Sept. 1990, pp. 456-463.

16. Pappa, R. S., "Eigensystem Realization Algorithm User's Guide for VAX/VMS Computers," NASA TM-109066, May 1994.

REPORT DOCUMENTATION PAGE

Form Approved
OMB No. 0704-0188

1. AGENCY USE ONLY *(Leave blank)*

2. REPORT DATE
November 1995

3. REPORT TYPE AND DATES COVERED
Technical Memorandum

4. TITLE AND SUBTITLE
Simulation of the Photogrammetric Appendage Structural Dynamics Experiment

5. FUNDING NUMBERS
WU 233-01-01-03

6. AUTHOR(S)
Richard S. Pappa, Michael G. Gilbert, and Sharon S. Welch

7. PERFORMING ORGANIZATION NAME(S) AND ADDRESS(ES)
NASA Langley Research Center
Hampton, VA 23681-0001

8. PERFORMING ORGANIZATION REPORT NUMBER

9. SPONSORING / MONITORING AGENCY NAME(S) AND ADDRESS(ES)
National Aeronautics and Space Administration
Washington, DC 20546-0001

10. SPONSORING / MONITORING AGENCY REPORT NUMBER
NASA TM - 110221

11. SUPPLEMENTARY NOTES
Will be presented at the 14th International Modal Analysis Conference in Dearborn, Michigan, on February 12-15, 1996.

12a. DISTRIBUTION / AVAILABILITY STATEMENT
Unclassified - Unlimited
Subject Category - 39

Availability: NASA CASI, (301) 621-0390

12b. DISTRIBUTION CODE

13. ABSTRACT *(Maximum 200 words)*
The Photogrammetric Appendage Structural Dynamics Experiment (PASDE) uses six video cameras in the Space Shuttle cargo bay to measure vibration of the Russian Mir space station Kvant-II solar array. It occurs on Shuttle/Mir docking mission STS-74 scheduled for launch in November 1995. The objective of PASDE is to demonstrate photogrammetric technology for measuring "untargeted" spacecraft appendage structural dynamics. This paper discusses a pre-flight simulation test conducted in July 1995, focusing on the image processing aspects. The flight camera system recorded vibrations of a full-scale structural test article having grids of white lines on black background, similar in appearance to the Mir solar array. Using image correlation analysis, line interesections on the structure are tracked in the video recordings to resolutions of less than 0.1 pixel. Calibration and mergng of multiple camera views generated 3-dimensional displacements from which structural modal parameters are then obtained.

14. SUBJECT TERMS
Photogrammetry, digital image processing, Space Station, structural dynamics measurements, modal identification, solar array vibration, spacecraft vibration

15. NUMBER OF PAGES
8

16. PRICE CODE
A02

17. SECURITY CLASSIFICATION OF REPORT	18. SECURITY CLASSIFICATION OF THIS PAGE	19. SECURITY CLASSIFICATION OF ABSTRACT	20. LIMITATION OF ABSTRACT
Unclassified	Unclassified		

NSN 7540-01-280-5500

Standard Form 298 (Rev. 2-89)
Prescribed by ANSI Std. Z39-18
298-102